ELSEVIER

Nanomedicine: Nanotechnology, Biology, and Medicine
11 (2015) 1077–1083

nanomedicine
Nanotechnology, Biology, and Medicine

nanomedjournal.com

Folic acid-tagged protein nanoemulsions loaded with CORM-2 enhance the survival of mice bearing subcutaneous A20 lymphoma tumors

Ana Loureiro, BSc[a,b], Gonçalo J.L. Bernardes, PhD[c,d,*], Ulyana Shimanovich, PhD[c], Marisa P. Sária, PhD[a,b], Eugénia Nogueira, MSc[a,b], Ana Preto, PhD[b], Andreia C. Gomes, PhD[b], Artur Cavaco-Paulo, PhD[a,**]

[a]*CEB–Centre of Biological Engineering, University of Minho, Campus of Gualtar, Braga, Portugal*
[b]*CBMA (Centre of Molecular and Environmental Biology), University of Minho, Campus of Gualtar, Braga, Portugal*
[c]*Department of Chemistry, University of Cambridge, Lensfield Road, Cambridge, United Kingdom*
[d]*Instituto de Medicina Molecular, Faculdade de Medicina da Universidade de Lisboa, Lisboa, Portugal*

Received 22 January 2015; accepted 24 February 2015

Abstract

Folic Acid (FA)-tagged protein nanoemulsions were found to be preferentially internalized on B-cell lymphoma cell line (A20 cell line), which, for the first time, is reported to express folate receptor (FR)-alpha. Carbon monoxide releasing molecule-2 (CORM-2) was incorporated in the oil phase of the initial formulation. FA-functionalized nanoemulsions loaded with CORM-2 exhibited a considerable antitumor effect and an increased survival of BALB/c mice bearing subcutaneous A20 lymphoma tumors. The developed nanoemulsions also demonstrated to be well tolerated by these immunocompetent mice. Thus, the results obtained in this study demonstrate that FA-tagged protein nanoemulsions can be successfully used in cancer therapy, with the important ability to delivery drugs intracellularly.

Key words: Protein nanoemulsions; Folic acid; CORM-2; Specific uptake; Targeted drug delivery

Background

Nanocarriers can modulate the pharmacokinetic and drug tissue distribution profile.[1,2] Specific anticancer drug delivery is promoted including targeting ligands,[1,3–5] such as folic acid (FA).[6] FA and FA conjugates bind with high affinity to folate receptor (FR)-alpha and -beta, and enter FR-expressing cells by receptor-mediated endocytosis.[7] FR-alpha expression is restricted to various normal epithelial cells, however it is overexpressed in several malignant cells and tissues.[8] FR-beta is a differentiation marker in normal hematopoiesis, being restricted to the myelomonocytic lineage and increasing during neutrophil maturation. FR-beta expression is also increased in activated monocytes/macrophages.[8] FA has emerged as an optimal targeting ligand with simple conjugation chemistry, non-immunogenicity and high affinity for the FR ($K_d = 10^{-10}$ M) even after conjugation.[9] Nanocarriers functionalized with FA are widely studied for cancer targeting aplications.

Carbon monoxide (CO) has shown beneficial effects in mammals.[10–13] CO can induce growth arrest of human cancer cells, as well as murine AC29 mesothelioma cells.[14] The first compound described as able to carry and deliver controlled

Author contributions: A.L. developed and optimized experimental protocols, performed experiments, analyzed and interpreted data and wrote the manuscript. E.N. and M.P.S. assisted in cellular experiments. U.S. performed 3D representation of nanoemulsions internalization by cells. G.J.L.B. designed the drug delivery and targeting system, performed *in vivo* experiments and assisted in writing the manuscript. A.C.G. and A.P. supervised all cellular experiments, analyzed and interpreted data and assisted in writing the manuscript. A.C.P. oversaw the project, analyzed and interpreted data and assisted in writing the manuscript.

Conflict of interest statement: None of the authors have any conflict to declare related to the study.

Sources of support: Ana Loureiro (SFRH/BD/81479/2011) and Eugénia Nogueira (SFRH/BD/81269/2011) hold scholarships from Fundação para a Ciência e a Tecnologia (FCT). Gonçalo J. L. Bernardes is a Royal Society University Research Fellow at the Department of Chemistry, University of Cambridge and an Investigador FCT at the Instituto de Medicina Molecular, Faculdade de Medicina da Universidade de Lisboa. This work has received funding from the European Union Seventh Framework Programme (FP7/2007-2013) under grant agreement NMP4-LA-2009-228827 NANOFOL. This work was supported by FEDER through POFC-COMPETE and by Portuguese funds from FCT through the project PEst-OE/BIA/UI4050/2014.

*Correspondence to: G.J.L. Bernardes, Department of Chemistry, University of Cambridge, Lensfield Road, Cambridge, CB2 1EW, United Kingdom.
**Corresponding author.
E-mail addresses: gb453@cam.ac.uk, gbernardes@medicina.ulisboa.pt (G.J.L. Bernardes), artur@deb.uminho.pt (A. Cavaco-Paulo).

http://dx.doi.org/10.1016/j.nano.2015.02.022
1549-9634/

quantities of CO in cellular systems was the tricarbonyldichlororuthenium(II) dimer ($[Ru(CO)_3Cl_2]_2$), known as CORM-2 (Carbon monoxide releasing molecule-2).[10,11,15–17] Ru has also been used independently in a variety of experimental anti-cancer drugs, with no acute or sub-acute toxicities reported.[15,18]

CORMs have been described as exhibiting a wide range of biological effects resulting in specific responses, which involve a restricted number of intracellular pathways and targets that encompass inflammation, apoptosis and cellular proliferation.[16] CORM-2, in particular, has been described to promote a beneficial therapeutic outcome in a number of mouse models of human disease.[15] However, CORM-2 has been shown to be highly unstable in plasma. Together with its observed anti-proliferative capacity,[19,20] this supports the advantage of targeted delivery of CORM-2 to cancer cells.

Here, we report the development of FA-tagged protein nanoemulsions loaded with CORM-2 for targeted drug delivery in a B-cell lymphoma model. Nanoemulsions were produced by high pressure homogenization of an aqueous phase (BSA solution containing a PEGylated surfactant and BSA–FA conjugate) with an organic phase (vegetable oil). Small, stable, PEGylated (described elsewhere[21]) and FA-functionalized nanoemulsions were obtained and evaluated in terms of specific uptake using a lymphoma cell line (A20 cell line). The biological effect of the nanoemulsions loaded with CORM-2 was tested both *in vitro* and *in vivo*. The results obtained suggest the use of FA-tagged protein nanoemulsions for targeted drug delivery in cancer therapy.

Methods

Nanoemulsion preparation

Nanoemulsions were prepared using a high pressure homogenizer (APV-2000, Denmark). BSA (Sigma-Aldrich, USA) and PEGylated surfactant (Sigma-Aldrich, USA) were dissolved in phosphate buffer saline (PBS), pH 7.4, at concentration of 10 mg/mL and 5 mg/mL, respectively. In this aqueous phase was also introduced a fluorescent agent using Fluorescein isothiocyanate (FITC) labeled-BSA (Sigma-Aldrich, USA) at a 1:20 ratio (m/m) relative to BSA protein. BSA–FA conjugate solution, previously prepared, was added at a 1:100 ratio (m/m) to the aqueous phase. The aqueous solution was emulsified with an organic solvent (vegetable oil) by subjecting the initial formulation to high pressure homogenization. The drug, CORM-2, was dissolved in vegetable oil phase.

Conjugation of FA with BSA

FA (Sigma-Aldrich, USA) dissolved in PBS, pH 7.4, was 'activated' with 5-fold excess of *N*-(3-dimethylaminopropyl)-*N*′-ethylcarbodiimide hydrochloride (Sigma-Aldrich, USA) and a 1-fold excess of *N*-hydroxysulfosuccinimide (Sigma-Aldrich, USA) for 2 h at room temperature. Activated FA was then added to BSA using a 75:1 FA to BSA moles ratio, and then left to react for 8-10 h. Dialysis against PBS was performed for 8 days in order to remove the excess FA and other reactants from the conjugated protein. The purified BSA–FA conjugate contained 35 mol of FA per 1 mol of BSA.

Physicochemical characterization

The size distribution and zeta-potential values of the nanoemulsions were determined at pH 7.4 (PBS buffer) and at 25 °C, using dynamic light scattering in a Malvern zetasizer NS, by photon correlation spectroscopy (PCS) and by electrophoretic laser Doppler anemometry, respectively. The values for viscosity and refractive index were taken as 0.890 cP and 1.330, respectively. The protein concentration was kept constant at 10 mg/mL.

Cells and culture conditions

B-cell lymphoma cell line (A20 cell line) (ATCC, TIB-208) was obtained from American Type Culture Collection (LGC Standards, UK).

The A20 cell line was grown in suspension in Petri dishes, which were not tissue culture treated (Sarstedt, Germany), using RPMI-1640 medium supplemented with 10% (v/v) of FBS; 1% (v/v) of penicillin/streptomycin solution; 2 mg/mL of sodium bicarbonate; and 0.05 mM of 2-mercaptoethanol. Exponentially growing culture was maintained in a humidified atmosphere of 5% CO_2 in air at 37 °C.

Protein extraction and Western blot analysis for FR confirmation in the A20 cell line

48 h-incubated cells (KB, A20 and K562 cell lines) were harvested, centrifuged at 2000 rpm (4 °C) for 10 min and washed in cold PBS. Following another centrifugation, at 6000 rpm (4 °C) for 3 min, cell pellets were resuspended, homogenized in 100 μl of ice-cooled radioimmunoprecipitation (RIPA) buffer (1% NP-40 in 150 mM NaCl, 50 mM Tris-HCl pH 7.5, 2 mM EDTA), supplemented with 20 mM NaF, 1 mM phenylmethylsulfonyl fuoride (PMSF), 20 mM Na2V3O4, a protease inhibitor cocktail (Roche, Germany), and then incubated for 10 min. The proteins were cleared by centrifugation at 10,000 × *g* (4 °C) for 10 min. The soluble protein concentration was determined using Bio-Rad DC protein assay (Bio-Rad Laboratories, USA). The BSA was considered as a control. 40 μg of the resulting cytosolic protein extracts was separated through 12% sodium dodecyl sulfate (SDS)-polyacrylamide gel electrophoresis, and transferred onto a Hybond®-P polyvinylidene difluoride membrane (GE Healthcare Life Sciences, USA). 5% (w/v) nonfat dry milk in PBS with 0.05% Tween-20 (TPBS) was used for blocking nonspecific protein binding. After 2 h of blocking incubation, the membrane was washed three times with TPBS. The membrane was then incubated overnight (4 °C) with primary antibody monoclonal rabbit to FA binding protein (Abcam®, United Kingdom), diluted in 1% BSA (w/v) in TBST (1:1000). Horseradish-peroxidase-conjugated secondary antibody (anti-rabbit IgG-HRP, Cell Signaling Technology Inc., USA) was diluted in 5% (w/v) nonfat dry milk in TBST (1:30,000). Subsequent membrane incubation (1 h, room temperature) was followed by three TPBS washes. Immobilon solutions (Millipore, USA) were used for chemiluminescent detection in the Chemi Doc XRS system. β-Actin was used as loading control.

Cell viability assay

A20 cell viability was studied using the Promega CellTiter 96® AQueous Non-Radioactive Cell Proliferation (MTS) assay (Promega, USA). Cells were seeded in 24-well tissue culture plates (Nunc, Denmark) at a density of 5×10^4 cells/well and co-incubated with treatment conditions for determined incubation times. After co-incubation, MTS was added and the cells were incubated for a further 4 h at 37 °C. After this period, the absorbance of the formazan product was read at 490 nm, using Spectra MAX 340PC microwell plate reader. Cell viability was expressed as a percentage relative to the negative control.

Uptake assay

Unbound BSA–FITC and BSA–FA were removed using Centricon tubes (Amicon Ultra-15, Millipore) and then the uptake of the nanoemulsions was evaluated. A20 cells were seeded at a density of 1×10^5 cells/well on coverslips pre-treated with Poly-L-lysine (Sigma-Aldrich, USA), and co-incubated with nanoemulsions for 4 h. Solutions of nanoemulsions were prepared in FA-free Hanks' Balanced Salt solution (HBSS medium) (Lonza, Belgium). Cells were washed with cold PBS and fixed with 500 μL of paraformaldehyde 4% (v/v) for 30 min and then permeabilized with Triton 0.1% (v/v) solution. After more two washing steps with PBS, cells were incubated with 5 U/mL of Alexa Fluor 568 Phalloidin (Molecular Probes by Life Technologies, USA). 2 μL of Permafluor (Thermo Scientific, United Kingdom) containing 5 μg/mL of Hoechst (Molecular Probes by Life Technologies, USA) was used for place coverslips on slides. Confocal observations were performed using an inverted Zeiss confocal laser scanning microscope (CLSM; Olympus Fluoview FV1000) and three dimensional models were produced, using the software Imaris image analysis program.

In vivo studies

All animal experiments were performed after institutional ethical approval and in agreement with national (Portuguese Veterinary Office) and international rules (FELASA; Federation of Laboratory Animal Science Associations) on animal welfare. Experiments were performed in agreement with Instituto de Medicina Molecular Ethical Regulations and the ethical approval was given under the project "Therapeutic evaluation of anti-cancer drugs in mouse models of cancer" licensed to Dr. Gonçalo Bernardes. Under those strict indications (3R's: reduce, replacement and refinement) the minimal number of animals calculated was 5 mice per group, which was considered sufficient for the purpose of this investigation. Immunocompetent 10-week-old female BALB/c mice were subcutaneously injected with A20 cells. BALB/c mice bearing subcutaneous A20 lymphoma tumors were treated intravenously with 200 μL of FA-functionalized nanoemulsions loaded CORM-2 (targeting FR), 200 μL of FA-functionalized nanoemulsions (carrying no drug), 200 μL of CORM-2 (non-targeted delivery of drug), or saline. The dose was chosen according to the safety profile already reported for CORM-2 in *in vivo* studies.[11] Therapy was initiated when tumors reached 80-120 mm^3 and a daily treatment was performed for 5 days. The mice were sacrificed once tumor reached a volume greater than 1000 mm^3, which is the general procedure for therapeutic assessment. The readout of the experiment is tumor volume which can be then translated into survival — survival here means the number of days mice took for tumors to reach a volume greater than 1000 mm^3. Mice body weight variations, during and after therapy, and survival curves for the different treatments applied were also determined.

Table 1
Conditions used for nanoemulsion preparation.

BSA solution/vegetable oil ratio (v/v)	99.5%/0.5%
BSA–FITC/BSA ratio (m/m)	1/20
BSA–FA conjugate/BSA ratio (m/m)	1/100
BSA/FA (mol/mol) in BSA–FA conjugate	1/35

Normal rodent feed contains a high concentration of FA (6 mg/kg feed), so mice were fed an FA-free diet (Harlan diet TD90261, Harlan Teklad) beginning 2 weeks before tumor implantation and maintained throughout the study in order to maintain serum FA concentrations closer to the range of normal human serum.[22,23] Being these mice most commonly used for evaluating the performance of most anticancer agents and the high FA levels in mice sera could negatively affect the performance of FA-drug formulations used for cancer therapy, the majority of "FA-targeted" pharmacological studies published had involved the use of animals that were acclimated to some form of low/free FA chow.[23,24]

Statistical analysis

Assumptions were met prior to data analysis. All data were tested for normality (Kolmogorov–Smirnov test) and homoscedasticity (Levene's test). To investigate the influence of PEGylated BSA nanoparticles with(out) CORM-2 on cell viability, a one-way ANOVA was conducted, with six levels: nanoemulsions, FA-nanoemulsions, nanoemulsions + CORM-2, FA-nanoemulsions + CORM-2, CORM-2 and death control (30% DMSO). Post hoc comparisons were conducted using Student–Newman–Keuls (SNK). A P value of 0.05 was used for significance testing. Analyses were performed in STATISTICA (StatSoft v.7, US).

Results

FA-tagged protein nanoemulsions and specific uptake by FR positive cells

We produced BSA nanoemulsions by high pressure homogenization of a BSA solution, containing a PEGylated surfactant, with vegetable oil (Table 1). The characterization of these protein nanoemulsions is presented in Table 2 and is in line with what was previously described by our group, demonstrating that the particles are small, neutral surface (zeta-potential close to zero) and present high stability along time.[21] All these results establish that these PEGylated protein nanoemulsions have suitable characteristics required for systemic administration. Nanoemulsions containing imaging and targeting agents were prepared by introducing of BSA–FITC and BSA–FA conjugate in aqueous phase of initial

Table 2
Characterization of nanoemulsions and FA-tagged nanoemulsions loaded with CORM-2.

	Z-average (d.nm)	Polydispersity index (PDI)	Zeta-potential (mV)	FA concentration (μg/L)
Nanoemulsions	93.7 (±8.2)	0.157 (±0.033)	−1.82 (±0.15)	–
FA-Nanoemulsions + CORM-2	90.9 (±5.1)	0.152 (±0.032)	−2.28 (±0.25)	449.3 (±19.7)

formulation (Table 1). To determine if FA at the nanoemulsion particle's surface promotes specific cell targeting and the endocytosis, the cellular uptake of nanoemulsions was evaluated in a B-cell lymphoma cell line (A20 cell line).

B-cell lymphoma is one of the most common hematologic malignancies and targeted therapy based on monoclonal antibodies has become a treatment of choice in the clinic. However, a substantial number of patients experience a clinical relapse as a consequence of poor or no response to the treatments.[25] Several new targeting ligands have recently emerged for B-cell lymphoma treatment.[26] We confirmed by western blot that FR-alpha is expressed in A20 cells (Figure 1, *A*), reported here for the first time. The KB cell line was used as FR positive control and K562 cell line as FR negative control.

The evaluation of specific cellular uptake of nanoemulsions was performed by confocal laser scanning microscopy. It was observed that FA-functionalized nanoemulsions are more efficiently internalized by A20 cells (Figure 1, *B*). These results suggest that FA-functionalized nanoemulsions interact efficiently with FR-alpha at the cellular surface and promote FR-mediated endocytosis. By staining with phalloidin, which is a high-affinity F-actin probe, we showed that the nanoparticles were indeed internalized by the A20 cells. 3D reconstructions of images obtained by confocal microscopy allowed determining the number of nanoparticles internalized per cell (Figure 1, *B*). We observed that, in average, approximately 7 fold more nanoparticles were internalized when FA is on the particle's surface.

FA-tagged protein nanoemulsions loaded with CORM-2 and specific drug delivery

We also evaluated the capacity of these BSA nanoemulsions for the selective delivery of drugs into FR expressing cells. We used CORM-2 as a model compound due to its described anti-proliferative capacity against cancer cells and its instability in plasma, which makes it an ideal candidate for encapsulation and targeted delivery. Taking into account the production method described, the prepared nanoemulsions are especially efficient for the entrapment of hydrophobic drugs, such as CORM-2. The physicochemical characterization of the nanoemulsions containing FA at the surface and CORM-2 encapsulated was performed and we observed that the values of size, polydispersity index (PDI) and zeta-potential are very similar to the values presented by the nanoemulsions (Table 2). The quantification of FA in these nanoemulsions was also performed using RIDASCREEN®FAST Folic acid test kit and the results showed a high concentration of FA at the surface of nanoemulsions (Table 2).

In order to understand the mechanism responsible for the CORM-2 induced anti-proliferative effect observed in A20 lymphoma cells (Figure 2, *A*), and taking into account the known link between CO and HO-1, we evaluated HO-1 expression and ROS levels in A20 exposed to different concentrations of CORM-2. We verified an increase of HO-1 protein expression in the presence of CORM-2, as reported in other pathologies (e.g. in kidney cells),[27] determined by Western blot analysis (Supporting information, Figure S1), however ROS production was not significantly altered (Supporting information, Figure S2).

FA-functionalized nanoemulsions loaded with CORM-2 were shown to have the same anti-proliferative effect than CORM-2 alone, which diffused across the cell membrane. This result demonstrated that these nanoemulsions recognized the FR present in surface of A20 cells, being internalized by FR-mediated endocytosis and releasing the drug, as intended. Additionally, the drug encapsulated in the nanoemulsions present several advantages for *in vivo* applications, as previously described. This decrease in cell proliferation is significantly different from the anti-proliferative effect observed for the empty nanoemulsions, whether FA-functionalized or not, and the non-targeted nanoemulsions containing CORM-2 ($F(5,12) = 138{,}304$, $P < 0.05$) (Figure 2, *B*). Nanoemulsions containing CORM-2, but not FA at the surface (non-targeted nanoemulsions), are not efficiently internalized by A20 cells and the drug remains protected, which explains the absence of anti-proliferative effect. These results suggest a preferential internalization of the FA-functionalized nanoemulsions by these FR positive cancer cells and also indicate an effective release of the drug from nanoemulsions *in vitro*.

The bioavailability and targeting specificity of these FA-functionalized PEGylated BSA nanoemulsions were also tested *in vivo*. Their therapeutic efficacy was tested in BALB/c mice bearing subcutaneous A20 lymphoma tumors. This syngeneic model mimics human disease in an immunocompetent host with aspects of diffuse large B-cell lymphomas,[28,29] which in our view is clinically relevant. The subcutaneous model has additional advantages, such as providing visual confirmation that mice do have tumors prior to therapy and easy assessment of tumor response or growth over time.[30]

Figure 3, *A* shows a considerable tumor growth inhibition when mice were treated with FA-functionalized nanoemulsions loaded with CORM-2, whilst empty FA-functionalized nanoemulsions were shown to have no effect. The treatment with FA-functionalized nanoemulsions containing CORM-2 substantially increased mice survival (Figure 3, *B*). The *in vivo* study also demonstrated that the disclosed PEGylated BSA nanoemulsions were well tolerated in immunocompetent mice, with no detectable weight loss (Figure 3, *C*).

Discussion

We have developed FA-functionalized BSA nanoemulsions that demonstrated specific drug delivery into FR positive cancer

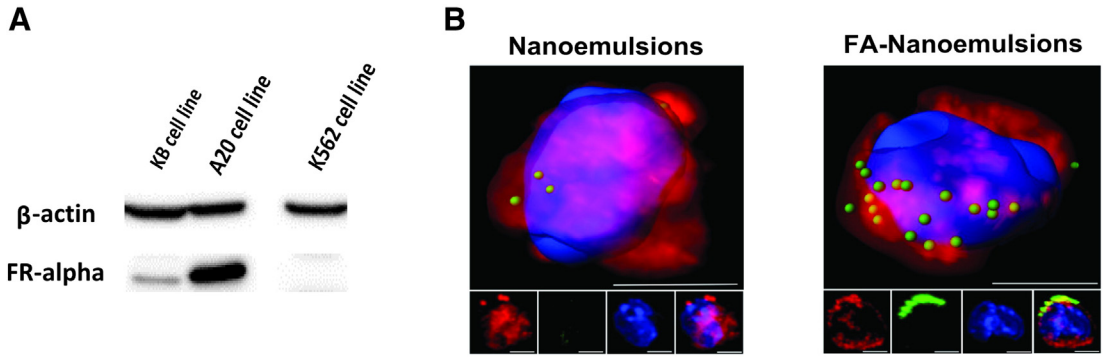

Figure 1. Evaluation of FA-tagged protein nanoemulsions using FR positive cancer cell line. **(A)** β-Actin and FR-alpha protein expression in KB, A20 and K562 cell lines analyzed by Western blot. **(B)** 3D representations of images obtained by confocal microscopy of nanoemulsions' internalization in A20 cell line, after 4 h of incubation (scale bars = 5 μm) (Blue = nuclear staining; Green = nanoemulsion particles; Red = phalloidin cytoskeleton staining).

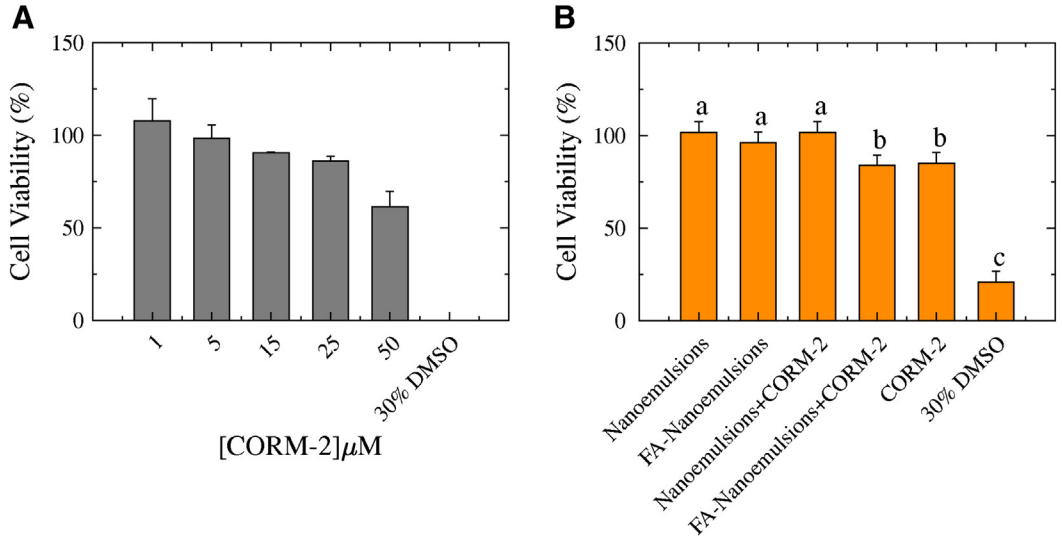

Figure 2. *In vitro* therapeutic efficacy of CORM-2 and FA-tagged protein nanoemulsions loaded with CORM-2 in A20 cell line. 30% (v/v) of DMSO was nominated as death control. To correct for variation, raw data were converted in percentage of cell viability, relative to the "cell-only" control. **(A)** A20 cell line viability after 48 h of contact with different concentrations of CORM-2. Values are the mean ± SEM of 2 independent experiments. **(B)** A20 cell line viability after 48 h of contact with 300 μg/mL of BSA nanoemulsions, with and without 6 μM of CORM-2 and the free-drug. Values are the mean ± SEM of 2 independent experiments. Different letters indicate significant differences among treatments ($P < 0.05$, one-way ANOVA).

cells. The expression of FR-alpha was confirmed in A20 B-cell lymphoma cells that were successfully targeted by FA-functionalized BSA nanoemulsions.

CORMs, as CO, induce specific biological responses, through activation of a few intracellular pathways and targets, regulating inflammation, apoptosis and cellular proliferation.[16] CO has the ability to block cancer cell proliferation.[11] It appears that CO exerts its effect through different pathways in different cell lines and under different conditions.[11,16] One of the central targets of CO seems to be the mithocondria and the overall bioenergetics of the cell. CO may promote mitochondrial biogenesis and drive mitochondria to increase ATP and ROS generation that in turn influences cellular behavior. Increasing ROS production would ultimately lead to induction of HO-1, which under certain circumstances may generate a positive feedback loop that contributes to the long-lasting beneficial effects of the HO1–CO pathway, perhaps involving other HO-1 products.[11] Our results indicate that in A20 cells, CORM-2 does in fact limit cell proliferation, possibly by involving HO-1 signaling but not affecting endogenous ROS levels.

The FA-tagged protein nanoemulsions loaded with CORM-2 led to considerable antitumor activity and the enhanced survival of mice bearing A20 lymphoma tumors. One possibility to explain this notable antitumor activity of FA-tagged nanoemulsions loaded with CORM-2 is the reported CO's anti-cancer effect as a result of inducing anti-Warburg effect.[14] The Warburg effect provides substrates for cell growth and division and free energy (adenosine triphosphate, ATP) from enhanced glucose uptake and elevated glycolysis with a limited oxygen

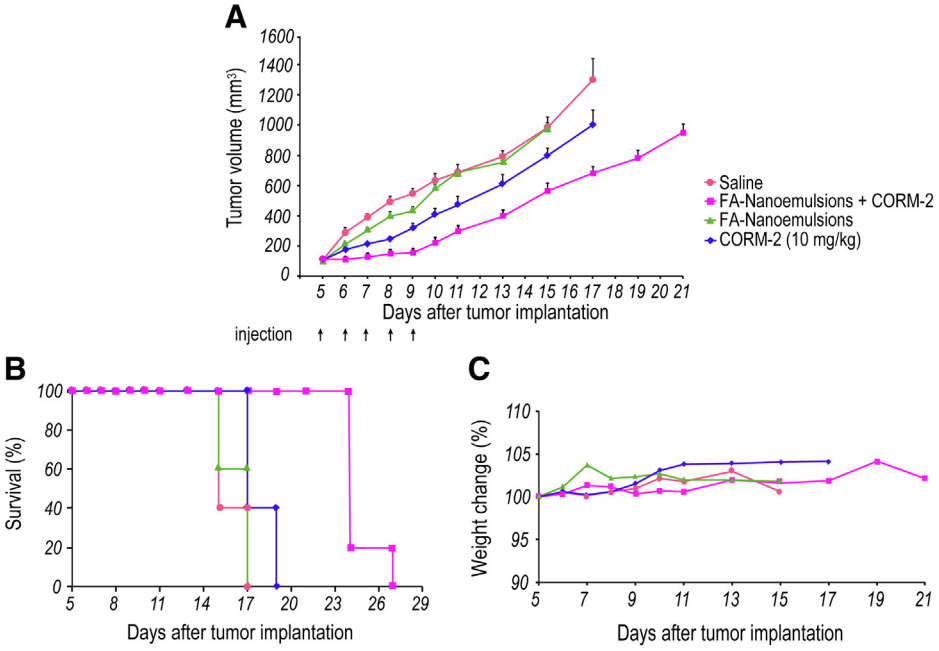

Figure 3. *In vivo* therapeutic efficacy of FA-tagged protein nanoemulsions loaded with CORM-2. **(A)** Tumor growth curves of immunocompetent 10-week-old female BALB/c mice bearing subcutaneous A20 lymphoma tumors treated intravenously with FA-functionalized nanoemulsions loaded CORM-2 (targeting FR), FA-functionalized nanoemulsions (carrying no drug), CORM-2 (non-targeted delivery of drug), or saline. Treatment was performed daily for a period of 5 days (arrows). Data represent mean tumor volumes (±SE). Tumor growth curves were stopped when tumors reached a size of 1000 mm^3. **(B)** Survival curves of mice treated with FA-functionalized nanoemulsions loaded CORM-2 and control groups. **(C)** Mice body weight variations during and after therapy.

consumption rate.[14,31] Exposure to CO uses this effect compelling the cancer cell to consume more oxygen that in turn drives metabolic demand, leading to growth inhibition, cellular exhaustion and death.[14]

In the present study we chose a syngeneic model of B-cell lymphoma in the BALB/c mouse, which mimics human disease in an immunocompetent host. The subcutaneous model presents advantages such as visual confirmation that mice used in an experiment have tumors prior to therapy; and assessment to tumor response or growth over time.[30] Subcutaneous models may however be promiscuous of small particle penetration.[32] Thus the effectiveness of targeting and effect over disease progression should be further supported, in future experiments *in vivo*, in an orthotopic fat-pad model or a disseminated lymphoma model to avoid this issue.

Small size, high stability over time, specific targeting capacity and non-immunogenicity support their application as drug delivery systems. Therefore, these novel FA-functionalized PEGylated BSA nanoemulsions are promising nanocarriers for the selective delivery of drugs to a target cell population that express FR. In this way, these functionalized nanocarriers may ameliorate the side effects and low efficacy of conventional cancer treatments. Furthermore, a number of new targeting ligands specific to B-cell lymphoma have been recently disclosed,[26] constituting attractive targets for building functionalized protein nanoemulsions for cancer drug delivery with maximum specificity.

Acknowledgments

We thank Ana Cristina Carvalho and Ana Oliveira for technical assistance in cellular experiments.

Appendix A. Supplementary data

Supplementary data to this article can be found online at http://dx.doi.org/10.1016/j.nano.2015.02.022.

References

1. Brigger I, Dubernet C, Couvreur P. Nanoparticles in cancer therapy and diagnosis. *Adv Drug Deliv Rev* 2012;**64**:24-36 [Supplement(0)].
2. Couvreur P, Vauthier C. Nanotechnology: intelligent design to treat complex disease. *Pharm Res* 2006;**23**(7):1417-50.
3. Peer D, Karp JM, Hong S, Farokhzad OC, Margalit R, Langer R. Nanocarriers as an emerging platform for cancer therapy. *Nat Nanotechnol* 2007;**2**:751-60.
4. Davis ME, Chen ZG, Shin DM. Nanoparticle therapeutics: an emerging treatment modality for cancer. *Nat Rev Drug Discov* 2008;**7**:771-82.
5. Krall N, Scheuermann J, Neri D. Small targeted cytotoxics: current state and promises from DNA-encoded chemical libraries. *Angew Chem Int Ed* 2013;**52**(5):1384-402.
6. Loureiro A, Abreu AS, Sarria MP, Figueiredo MCO, Saraiva LM, Bernardes GJL, et al. Functionalized protein nanoemulsions by incorporation of chemically modified BSA. *RSC Adv* 2015;**5**(7):4976-83.

7. Low PS, Kularatne SA. Folate-targeted therapeutic and imaging agents for cancer. *Curr Opin Chem Biol* 2009;**13**:256-62.
8. Elnakat H, Ratnam M. Distribution, functionality and gene regulation of folate receptor isoforms: implications in targeted therapy. *Adv Drug Deliv Rev* 2004;**56**(8):1067-84.
9. Low PS, Henne WA, Doorneweerd DD. Discovery and development of folic-acid-based receptor targeting for imaging and therapy of cancer and inflammatory diseases. *Acc Chem Res* 2007;**41**(1):120-9.
10. Foresti R, Bani-Hani M, Motterlini R. Use of carbon monoxide as a therapeutic agent: promises and challenges. *Intensive Care Med* 2008;**34**(4):649-58.
11. Motterlini R, Otterbein LE. The therapeutic potential of carbon monoxide. *Nat Rev Drug Discov* 2010;**9**(9):728-43.
12. Nikolic I, Saksida T, Mangano K, Vujicic M, Stojanovic I, Nicoletti F, et al. Pharmacological application of carbon monoxide ameliorates islet-directed autoimmunity in mice via anti-inflammatory and anti-apoptotic effects. *Diabetologia* 2014;**57**(5):980-90.
13. Fagone P, Mangano K, Quattrocchi C, Motterlini R, Di Marco R, Magro G, et al. Prevention of clinical and histological signs of proteolipid protein (PLP)-induced experimental allergic encephalomyelitis (EAE) in mice by the water-soluble carbon monoxide-releasing molecule (CORM)-A1. *Clin Exp Immunol* 2011;**163**(3):368-74.
14. Wegiel B, Gallo D, Csizmadia E, Harris C, Belcher J, Vercellotti GM, et al. Carbon monoxide expedites metabolic exhaustion to inhibit tumor growth. *Cancer Res* 2013;**73**(23):7009-21.
15. Romao CC, Blattler WA, Seixas JD, Bernardes GJL. Developing drug molecules for therapy with carbon monoxide. *Chem Soc Rev* 2012;**41**(9):3571-83.
16. Knauert M, Vangala S, Haslip M, Lee PJ. Therapeutic applications of carbon monoxide. *Oxid Med Cell Longev* 2013;**2013**:11.
17. García-Gallego S, Bernardes GJL. Carbon-monoxide-releasing molecules for the delivery of therapeutic CO in vivo. *Angew Chem Int Ed* 2014;**53**(37):9712-21.
18. Levina A, Mitra A, Lay PA. Recent developments in ruthenium anticancer drugs. *Metallomics* 2009;**1**(6):458-70.
19. Motterlini R, Clark JE, Foresti R, Sarathchandra P, Mann BE, Green CJ. Carbon monoxide-releasing molecules: characterization of biochemical and vascular activities. *Circ Res* 2002;**90**(2):e17-24.
20. Winburn IC, Gunatunga K, McKernan RD, Walker RJ, Sammut IA, Harrison JC. Cell damage following carbon monoxide releasing molecule exposure: implications for therapeutic applications. *Basic Clin Pharmacol Toxicol* 2012;**111**(1):31-41.
21. Nogueira E, Loureiro A, Nogueira P, Freitas J, Almeida CR, Harmark J, et al. Liposome and protein based stealth nanoparticles. *Faraday Discuss* 2013;**166**:417-29.
22. Mathias CJ, Wang S, Lee RJ, Waters DJ, Low PS, Green MA. Tumor-selective radiopharmaceutical targeting via receptor-mediated endocytosis of gallium-67-deferoxamine-folate. *J Nucl Med* 1996;**37**(6):1003-8.
23. Leamon CP, Reddy JA, Dorton R, Bloomfield A, Emsweller K, Parker N, et al. Impact of high and low folate diets on tissue folate receptor levels and antitumor responses toward folate-drug conjugates. *J Pharmacol Exp Ther* 2008;**327**(3):918-25.
24. Gautam N, Puligujja P, Balkundi S, Thakare R, Liu X-M, Fox HS, et al. Pharmacokinetics, biodistribution, and toxicity of folic acid-coated antiretroviral nanoformulations. *Antimicrob Agents Chemother* 2014;**58**(12):7510-9.
25. Palmieri C, Falcone C, Iaccino E, Tuccillo FM, Gaspari M, Trimboli F, et al. In vivo targeting and growth inhibition of the A20 murine B-cell lymphoma by an idiotype-specific peptide binder. *Blood* 2010;**116**(2):226-38.
26. Reeder CB, Ansell SM. Novel therapeutic agents for B-cell lymphoma: developing rational combinations. *Blood* 2011;**117**(5):1453-62.
27. Sun B, Sun Z, Jin Q, Chen X. CO-releasing molecules (CORM-2)-liberated CO attenuates leukocytes infiltration in the renal tissue of thermally injured mice. *Int J Biol Sci* 2008;**4**(3):176-83.
28. Passineau MJ, Siegal GP, Everts M, Pereboev A, Jhala D, Wang M, et al. The natural history of a novel, systemic, disseminated model of syngeneic mouse B-cell lymphoma. *Leuk Lymphoma* 2005;**46**(11):1627-38.
29. Donnou S, Galand C, Touitou V, Sautès-Fridman C, Fabry Z, Fisson S. Murine models of B-cell lymphomas: promising tools for designing cancer therapies. *Adv Hematol* 2012;**2012**, http://dx.doi.org/10.1155/2012/701704.
30. Huynh AS, Abrahams DF, Torres MS, Baldwin MK, Gillies RJ, Morse DL. Development of an orthotopic human pancreatic cancer xenograft model using ultrasound guided injection of cells. *PLoS One* 2011;**6**(5):e20330.
31. Levine AJ, Puzio-Kuter AM. The control of the metabolic switch in cancers by oncogenes and tumor suppressor genes. *Science* 2010;**330**(6009):1340-4.
32. Chrastina A, Massey KA, Schnitzer JE. Overcoming in vivo barriers to targeted nanodelivery. *Wiley Interdiscip Rev Nanomed Nanobiotechnol* 2011;**3**(4):421-37.